Early stages of radiation damage in graphite and carbon nanostructures: A first-principles molecular dynamics study

Oleg V. Yazyev,* Ivano Tavernelli, Ursula Rothlisberger, and Lothar Helm
Ecole Polytechnique Fédérale de Lausanne (EPFL), Institute of Chemical Sciences and Engineering, CH-1015 Lausanne, Switzerland
(Received 28 December 2006; published 19 March 2007)

Understanding radiation-induced defect formation in carbon materials is crucial for nuclear technology and for the manufacturing of nanostructures with desired properties. Using first-principles molecular dynamics, we perform a systematic study of the nonequilibrium processes of radiation damage in graphite. Our study reveals a rich variety of defect structures (vacancies, interstitials, intimate interstitial-vacancy pairs, and in-plane topological defects) with formation energies of 5–15 eV. We clarify the mechanisms underlying their creation and find unexpected preferences for particular structures. Possibilities of controlled defect-assisted engineering of nanostructures are analyzed. In particular, we conclude that the selective creation of two distinct low-energy intimate Frenkel pair defects can be achieved by using a 90–110 keV electron beam irradiation.

DOI: 10.1103/PhysRevB.75.115418 PACS number(s): 61.72.Ji, 61.80.Az, 81.05.Uw

I. INTRODUCTION

Radiation resistance of graphite has been one of the major concerns of the nuclear industry.[1,2] Nowadays, radiation treatment by high-energy electrons or ions is also viewed as a versatile tool for the design of new materials. The formation of irradiation-induced defects in graphitelike layered carbon nanostructures (multiwalled and bundled carbon nanotubes, nanoonions, etc.) changes their mechanical[3] and electronic properties[4,5] and may even trigger dramatic structural changes.[6,7] However, the structure and dynamics of defects in graphite and carbon nanostructures as well as the mechanisms underlying their creation and transformation remain elusive. This knowledge is crucial for a defect-assisted engineering of nanostructures with applications in, e.g., manufacturing of nanoelectromechanical systems.[8]

Radiation damage of matter is governed by the displacement of atoms from their equilibrium positions due to electronic excitations and direct collisions of high-energy particles with the nuclei. In metals and narrow band gap semiconductors electronic excitations quench instantaneously, leaving collisions with nuclei as the sole mechanism responsible for the creation of defects in graphite and related carbon materials.[9] If the kinetic energy transferred from a high-energy electron or ion to the nucleus is higher than the displacement threshold T_d, a carbon atom can leave its initial position to form a metastable defect structure on a subpicosecond time scale. Such events are called knock-on displacements. For highly anisotropic layered carbon materials the threshold of the off-plane displacement is $T_d^{\perp} \approx 15-20$ eV,[6] while a creation of defect due to the in-plane knock-on collision requires higher transferred energies, $T_d^{\parallel} \geqslant 30$ eV. Possible defects produced by radiation damage include separated and intimate[10] pairs of interstitial atoms and vacancies, and in-plane topological defects involving non-sixmembered rings, e.g., Stone-Wales defect.[11,12] The existence of defects in carbon nanostructures has been confirmed by direct observations.[13,14]

Upon knock-on events a large amount of energy is transferred to only a few degrees of freedom. The resulting defect structures formed on a picosecond time scale depend on the magnitude and on the direction of the transferred momentum and determine the fate of the system at longer time scales. Therefore gaining control over the early stages of defect formation by tuning the irradiation conditions will make the paradigm of the defect-assisted engineering feasible. Molecular dynamics (MD) simulations performed with empirical potentials[15] or tight-binding models[16–18] have been used for the studies of radiation damage of various carbon materials.

In this work, we report a *systematic first-principles* study of the early stages of radiation damage of graphite, a general model for closely related layered carbon nanostructures. The paper is organized in the following way: In Sec. II we provide a description of the computational methods used in this work. The observed defect structures, mechanisms of their formation, and practical implications are discussed in Sec. III. Section IV briefly concludes our work.

II. COMPUTATIONAL METHODS

By using *ab initio* molecular dynamics we simulate the process of defect formation after the initial transfer of a momentum $\vec{T}$ to one of the carbon atoms in the system. The periodic model system consists of a unit cell with 108 carbon atoms, which contains two graphene sheets with stacking ABAB. The dimension of the unit cell in the direction perpendicular to the graphene planes was fixed to 6.7 Å in accordance with the experimental interlayer distance 3.35 Å.[19] This distance shows only weak variation among different layered carbon nanostructures. Our computational methodology is based on density functional theory (DFT), which lacks a correct description of weak van der Waals interactions between graphene planes. However, by fixing the unit cell dimension in the direction perpendicular to the graphene planes we provide a realistic description of layered carbon nanostructures without any explicit inclusion of van der Waals forces. The in-plane distance between two periodic images is 12.7 Å which is large enough to ensure localization of the defect within the unit cell. A coarse sampling of the irreducible wedge of the space spanned by the magnitude

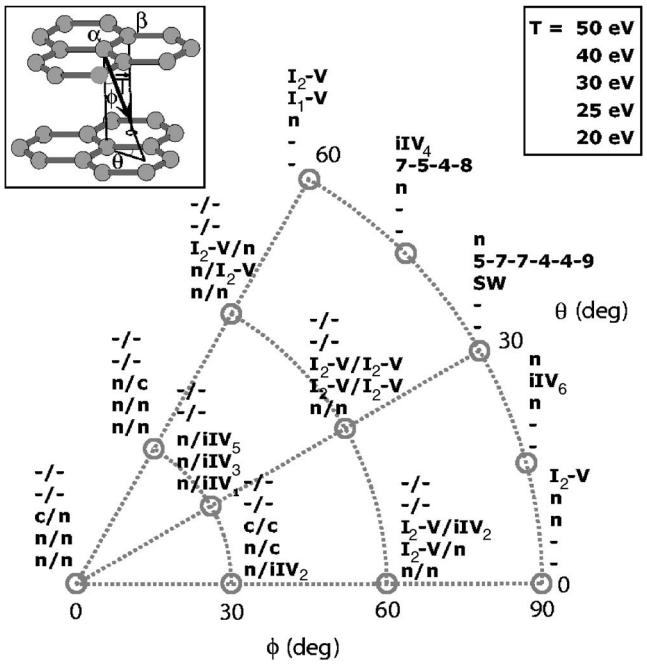

FIG. 1. Polar coordinates representation of the simulation outcomes as a function of the parameters T, ϕ, and θ. The defect structures at each parameter set are given according to the nomenclature shown in Figs. 2 and 4. Other labels correspond to "n" –no defect formation, "c" –displacement cascade, and "–" –simulation not performed. The different outcomes corresponding to the off-plane displacements of α/β carbon atoms (see left inset) are shown separately. For each pair of parameters (ϕ, θ) the outcomes at different values of T are listed according to the values given in the right inset. The left inset shows the definition of the parameters determining the knock-on displacements.

of transferred energy T and the pair of angles $\phi \in [0°;90°]$ and $\theta \in [0°;60°]$ (Fig. 1, inset) has been performed.

The *ab initio* MD simulations were carried out using the CPMD plane wave DFT code[20] and the Perdew, Burke, and Ernzerhof exchange-correlation density functional.[21] A plane wave kinetic energy cutoff of 60 Ry and norm-conserving pseudopotentials[22] have been used. The simulations were performed within the spin-unrestricted formulation of DFT starting from an initial guess asymmetric with respect to the spin components. Such a starting configuration is required in order to ensure a broken-symmetry path of bond breaking events.[23] The first 100 fs of each MD simulation were performed using the Born-Oppenheimer scheme. The MD time step was set to 0.5 fs. In our simulations we observed that during the first 100 fs the transferred kinetic energy was well-dissipated over the entire system. The initial simulation was followed by a Car-Parrinello simulation[24] carried out using a Nosé-Hoover thermostat[25] (350 K) until a stable defect structure was reached (about 1 ps). This thermal coupling methodology provides a realistic description of the excess kinetic energy dissipation after knock-on collisions of reasonably low transferred energies. The Car-Parrinello equations of motion were integrated with a time step of 0.1 fs using a fictitious electron mass of 400 a.u. Finally, the obtained defect structures were relaxed by slow annealing of both ionic and electronic degrees of freedom.

The formation energies were evaluated using the SIESTA code[26] by relaxing the ionic coordinates and the in-plane cell dimensions. The same norm-conserving pseudopotentials and density functional as in the plane wave calculations together with an optimized double-ζ plus polarization function (DZP) basis set were used. A $2\times2\times2$ k-point grid (including the Γ point) was employed in order to obtain accurate defect formation energies.[27]

III. RESULTS AND DISCUSSION

A. Off-plane recoils

The outcomes of our simulations are summarized in Fig. 1 (movies of selected MD trajectories are available online[28]). We first discuss the simulation results for the off-plane displacements ($\phi \in \{0°;30°;60°\}$) of carbon atoms in inequivalent positions α and β. The outcomes can be divided into four major classes: (i) no defect formation due to insufficient transferred momentum or due to instantaneous recombination of the recoil atom with the vacancy ("n"); (ii) separated interstitial-vacancy pairs (*I-V*); (iii) intimate interstitial-vacancy pairs (*iIV*); and (iv) displacement cascades ("c") in which the recoil atom is able to displace other atoms in the lattice. The latter case can be viewed as a series of elementary events of types (i)–(iii). The simulation of displacement cascades is beyond the scope of this study and would require a larger unit cell than the one used here.

The formation of well-separated Frenkel pairs was observed for atoms in both α and β positions at $T \geqslant 25$ eV. Surprisingly, the interstitial defects were produced only in the form of a symmetric "dumbell" structure (I_2)[29,30] where the two carbon atoms are symmetrically displaced from the graphene plane (Fig. 2, top). Despite the highly distorted coordination sphere of these atoms, the C-C distance of 1.58 Å is close to the one of a typical σ bond. The core atomic structure is the same as for the [1.1.1]propellane molecule for which a very similar C-C bond length (1.60±0.02 Å) has been observed experimentally.[31] No single off-plane recoil led to the "bridge" structure (I_1)[15,29,32] with the interstitial atom situated between two graphene planes. The formation energy of I_2 (E_f=14.3 eV, the value refers to the formation energy of the corresponding *I-V* pair) is only 0.5 eV lower than the one of I_1 (E_f=14.8 eV) where the "bridge" interstitial defect is bonded only to the neighbor atoms in the same layer. In this case, a steric repulsion with the opposite graphene layer contributes to the destabilization of the I_1 defect. However, bonding to the opposite layer leads to more stable shared interstitial defect structures.[2,29] In the ylid (E_f=14.1 eV) and spiro (E_f=13.1 eV) configurations, the shared interstitial atom is additionally bound to one and, respectively, to two carbon atoms of the adjacent layer. These structures have not been observed in our MD simulations. The observed preference for the I_2 configuration in graphite may have the following origin. In the "dumbell" configuration the recoil atom is able to transfer its excess kinetic energy to the other atoms more efficiently than in the

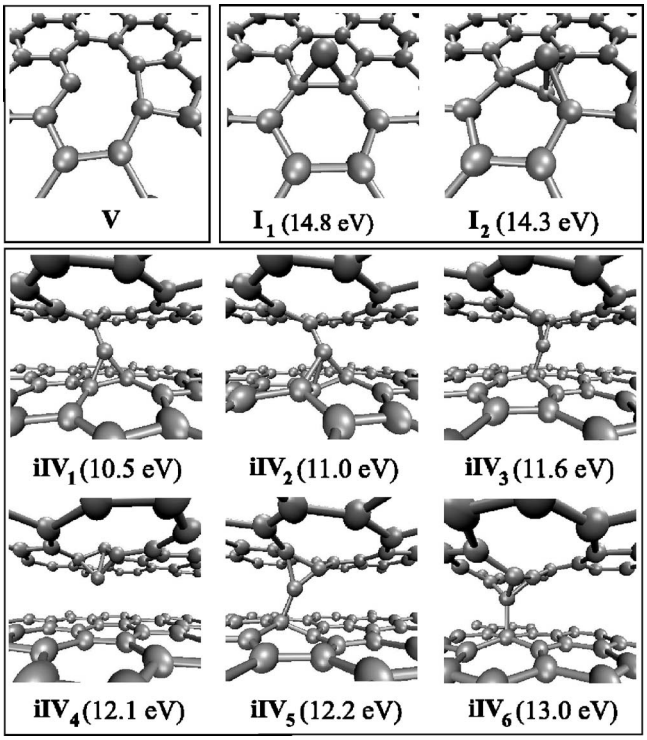

FIG. 2. Perspective views of the atomic structures of the vacancy (top, left), interstitial (top, right), and intimate Frenkel pair (bottom) defects observed in our simulations. The formation energies are given in parentheses. The values given for interstitial defects refer to the formation energies of corresponding Frenkel pairs. For *iIV* defects the created vacancy is situated in the upper graphene layer.

case of the "bridge" configuration. At the same time, the formation of shared interstitials requires the improbable collective motion of a number of atoms in the two adjacent graphene layers in the direction of the recoil atom. This explains the observed high probability for the formation of the I_2 defect structure in the early stages of the radiation-induced defect formation. For the isolated graphene sheet, I_1 is 0.2 eV more stable than I_2 due to the absence of the steric repulsion with the adjacent graphene layer. In curved graphenic structures, like carbon nanotubes, the "bridge" interstitial defect undergoes further stabilization. Our first-principles calculations predict that the transition from the defect structure I_2 to the structure I_1 in graphite is characterized by an activation barrier of 0.9 eV. The "dumbell" interstitial can also be viewed as a stable intermediate of the self-diffusion process in graphite along the *c*-axis, occurring via the substitution of a carbon atom in the graphene layer.[33] The energy diagram for the diffusion process along the *c*-axis is shown in Fig. 3.

Formation of intimate interstitial-vacancy pairs (*iIV*) requires lower transferred kinetic energies. At $T=20$ eV we observed the formation of two low energy *iIV* pairs, iIV_1 ($E_f=10.5$ eV) and iIV_2 ($E_f=11.0$ eV) (Fig. 2, bottom). The displaced atom bridges the defect vacancy with two, respectively, three neighbor atoms in the opposite layer, which undergo rehybridization. A fine scan of the transferred momentum space indicates a T_d value of 18 eV for graphite, in

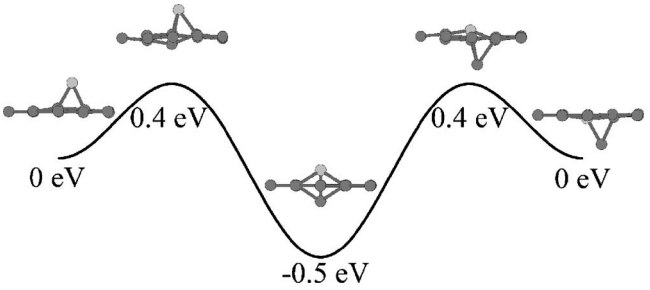

FIG. 3. The scheme of the self-diffusion process in graphite along the *c*-axis. The diffusing carbon adatom (highlighted in the figure) substitutes one of the carbon atoms in the graphite layer. The relative energies of local minima and transition states are shown.

agreement with other reported values.[6,34] As a consequence, the use of a particle beam energy capable of achieving a maximum kinetic energy transfer just above T_d will *selectively* create *iIV* defects. This value for T_d would correspond to the maximum kinetic energy transferred by an electron beam of 90 keV.[34] In the case of carbon nanotubes, T_d is expected to be lower due to curvature effects.[14] This proves the crucial role of the *iIV* defects in the reinforcement of carbon nanotube bundles[3,35] produced by 80 keV electron irradiation. Our results suggest the optimal conditions for the modification of mechanic and electronic properties of carbon-based layered nanostructures by means of the formation of *iIV* defects. For graphite and closely related nanostructures, electron beam acceleration voltages of 90–110 kV can be used. Such modifications are nondestructive since *iIV* defects tend to self-recombine without producing extensive damage of the nanostructure.[14] This is also supported by the fact that the barriers for iIV_1 defect recombination[10] and for the transformation of iIV_1 into iIV_2 (0.9 eV in this study) lie below the formation energies of *I-V* pairs.

Our computed formation energy for the previously proposed iIV_1 structure[10] is in good agreement with the values reported in other studies.[10,29,35] However, MD simulations on a longer time scale indicate that the asymmetric iIV_1 defect in graphite is not stable against recombination at 350 K if the shear of neighboring graphite layers is allowed. By contrast, the symmetric iIV_2 defect is stable throughout our MD simulations. Two other intimate Frenkel pairs, iIV_3 ($E_f=11.6$ eV) and iIV_5 ($E_f=12.2$ eV) have been obtained upon off-plane recoils caused by larger transferred momenta. In both structures the displaced carbon atom is linked to two carbon atoms in its host layer and one atom in the neighboring layer. It is notable that the formation of *iIV* defects has been observed *only* upon recoil of the β carbon atom. We explain this observation by the large probability of instantaneous recombination of the α atom recoils due to the local arrangement of atoms in the adjacent layer.

B. In-plane recoils

The formation of defects after displacement in the graphene plane ($\phi=90°$) requires higher transferred energies $T \geqslant 30$ eV. At $T=30$ eV ($\theta=30°$) we observed the formation

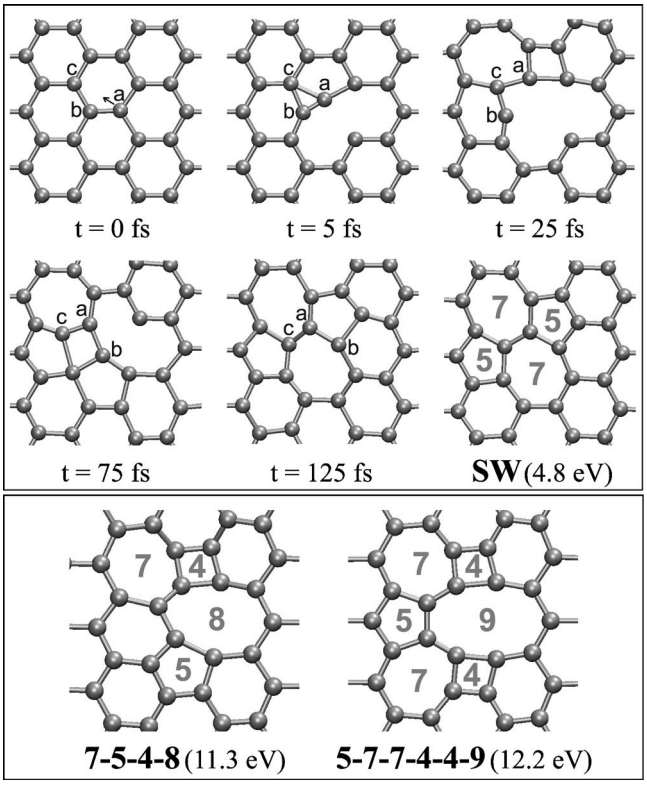

FIG. 4. Top: The mechanism of formation of a Stone-Wales defect upon in-plane knock-on displacement (T=30 eV). The carbon atoms involved in the rearrangement are marked with letters. Bottom: Atomic structures of 7-5-4-8 and 5-7-7-4-4-9 topological defects (arabic numbers indicate non-sixmembered rings).

of a Stone-Wales (SW) defect,[11] which is the lowest energy (E_f=4.8 eV) defect in graphite. The mechanism of its formation involves the cyclic permutation of three carbon atoms occurring during the first 100 fs after the knock-on collision (Fig. 4, top). A much lower activation barrier of ≈10 eV is required when the SW defect is formed upon simultaneous in-plane rotation of two neighboring carbon atoms.[12] However, this mechanism *cannot* be realized upon knock-on collisions because in this case the kinetic energy is transferred to a single atom. Irradiation of graphene-based materials, using an electron beam of energy just above 150 keV and oriented along the graphene plane, will result in an *increase* of yield of SW defects. This can be used for tuning electronic properties of materials.[36] However, because of the high energy transfer required for their formation, SW defects will be accompanied by the formation of Frenkel pairs, which form upon low energy ($T<30$ eV) off-plane recoils.

For $T>30$ eV two possible general mechanisms of defect formation have been identified. The first one involves the formation of strained structures containing non-sixmembered rings, which have formation energies higher than the formation energy of the SW defect. Two such structures, 7-5-4-8 (E_f=11.3 eV) and 5-7-7-4-4-9 (E_f=12.2 eV) have been observed in our simulations (Fig. 4, bottom). The second mechanism involves the expulsion of one carbon atom from the graphene plane shortly after the collision. In this case interstitial-vacancy pairs are formed. We observed formation of the "bridge" interstitial defect I_1 caused by the expulsion of a carbon atom with low kinetic energy. In addition, two new intimate interstitial-vacancy pairs, iIV_4 (E_f=12.1 eV) and iIV_6 (E_f=13.0 eV) have been characterized. In the iIV_4 structure the defect is localized in the graphene layer where the collision took place. On the contrary, the displaced carbon atom in the iIV_6 structure bridges three atoms of its host layer with one of the neighboring layers. The formation energies of all six *iIV* structures found in our simulations lie within a narrow interval of 2.5 eV, and they are all below the formation energies of separated *I-V* pairs. These defects should be stable at long time scales and at moderate temperatures.

IV. CONCLUSIONS

In conclusion, we performed an *ab initio* molecular dynamics study of radiation-induced defect formation in graphite. A variety of different defects, including structures which have never been discussed previously, were observed in our simulations. The produced defects depend strongly upon the direction and magnitude of the transferred momentum, resulting in the selective formation of certain defect structures. We showed the crucial role played by the early stage dynamics in the defect formation process, and we identified the conditions at which selective creation of defects can be achieved. In particular, we identified an interval of electron beam energies at which only low-energy intimate Frenkel pair defects bridging adjacent graphene layers are produced. We also conclude that Stone-Wales defects, characterized by the lowest formation energy, cannot be produced selectively upon irradiation. Our results are of practical importance for radiation-assisted manufacturing of carbon materials and nanostructures with new desired properties and functions.

ACKNOWLEDGMENTS

The authors acknowledge L. Forró, A. Kis, A. Kulik, S. Reich, B. I. Yakobson, and A. Zettl for discussions. O.Y. thanks the Swiss NSF for financial support. The computational resources were provided by the CSCS and the DIT-EPFL.

*Electronic address: oleg.yazyev@epfl.ch

[1] J. H. W. Simmons, *Radiation Damage in Graphite* (Pergamon, London, 1965).

[2] R. H. Telling, C. P. Ewels, A. A. El-Barbary, and M. I. Heggie, Nat. Mater. **2**, 333 (2003).

[3] A. Kis, G. Csányi, J.-P. Salvetat, T.-N. Lee, E. Couteau, A. J. Kulik, W. Benoit, J. Brugger, and L. Forró, Nat. Mater. **3**, 153 (2004).

[4] C. Mikó, M. Milas, J. W. Seo, E. Couteau, N. Barisic, R. Gaál, and L. Forró, Appl. Phys. Lett. **83**, 4622 (2003).
[5] K.-H. Han, D. Stepmann, P. Esquinazi, R. Höhne, V. Riede, and T. Butz, Adv. Mater. (Weinheim, Ger.) **15**, 1719 (2003).
[6] F. Banhart, J. Appl. Phys. **81**, 3440 (1997).
[7] M. Terrones, H. Terrones, F. Banhart, J.-C. Charlier, and P. M. Ajayan, Science **288**, 1226 (2000).
[8] J. Cummings and A. Zettl, Science **289**, 602 (2000); A. M. Fennimore, T. D. Yuzvinsky, W.-Q. Han, M. S. Fuhrer, J. Cumings, and A. Zettl, Nature (London) **424**, 408 (2003); K. Jensen, Ç. Girit, W. Mickelson, and A. Zettl, Phys. Rev. Lett. **96**, 215503 (2006); A. Kis, K. Jensen, S. Aloni, W. Mickelson, and A. Zettl, *ibid.* **97**, 025501 (2006).
[9] F. Banhart, Rep. Prog. Phys. **62**, 1181 (1999).
[10] C. P. Ewels, R. H. Telling, A. A. El-Barbary, M. I. Heggie, and P. R. Briddon, Phys. Rev. Lett. **91**, 025505 (2003).
[11] A. J. Stone and D. J. Wales, Chem. Phys. Lett. **128**, 501 (1986).
[12] E. Kaxiras and K. C. Pandey, Phys. Rev. Lett. **61**, 2693 (1988).
[13] A. Hashimoto, K. Suenaga, A. Gloter, K. Urita, and S. Iijima, Nature (London) **430**, 870 (2004).
[14] K. Urita, K. Suenaga, T. Sugai, H. Shinohara, and S. Iijima, Phys. Rev. Lett. **94**, 155502 (2005).
[15] K. Nordlund, J. Keinonen, and T. Mattila, Phys. Rev. Lett. **77**, 699 (1996).
[16] V. H. Crespi, N. G. Chopra, M. L. Cohen, A. Zettl, and S. G. Louie, Phys. Rev. B **54**, 5927 (1996).
[17] A. V. Krasheninnikov, F. Banhart, J. X. Li, A. S. Foster, and R. M. Nieminen, Phys. Rev. B **72**, 125428 (2005).
[18] P. M. Ajayan, V. Ravikumar, and J.-C. Charlier, Phys. Rev. Lett. **81**, 1437 (1998).
[19] M. Hanfland, H. Beister, and K. Syassen, Phys. Rev. B **39**, 12598 (1989).
[20] CPMD version 3.9.1, Copyright IBM Corp. 1990–2004, Copyright MPI für Festkörperforschung Stuttgart 1997–2001, http://www.cpmd.org.
[21] J. P. Perdew, K. Burke, and M. Ernzerhof, Phys. Rev. Lett. **77**, 3865 (1996).
[22] N. Troullier and J. L. Martins, Phys. Rev. B **43**, 1993 (1991).
[23] O. Gunnarsson and B. I. Lundquis, Phys. Rev. B **13**, 4274 (1976).
[24] R. Car and M. Parrinello, Phys. Rev. Lett. **55**, 2471 (1985).
[25] S. Nosé, J. Chem. Phys. **81**, 511 (1984); S. Nosé, Mol. Phys. **52**, 255 (1984); W. G. Hoover, Phys. Rev. A **31**, 1695 (1985).
[26] J. M. Soler, E. Artacho, J. D. Gale, A. García, J. Junquera, P. Ordejón, and D. Sánchez-Portal, J. Phys.: Condens. Matter **14**, 2745 (2002).
[27] C. G. Van de Walle and J. Neugebauer, J. Appl. Phys. **95**, 3851 (2004).
[28] See EPAPS Document No. E-PRBMDO-75-057711 for animation sequences of selected MD simulations. For more information on EPAPS, see http://www.aip.org/pubservs/epaps.html.
[29] L. Li, S. Reich, and J. Robertson, Phys. Rev. B **72**, 184109 (2005).
[30] Y. Ma, A. S. Foster, A. V. Krasheninnikov, and R. M. Nieminen, Phys. Rev. B **72**, 205416 (2005).
[31] K. B. Wiberg, W. P. Dailey, F. H. Walker, S. T. Waddell, L. S. Cracker, and M. Newton, J. Am. Chem. Soc. **107**, 7241 (1985).
[32] P. O. Lehtinen, A. S. Foster, A. Ayuela, A. Krasheninnikov, K. Nordlund, and R. M. Nieminen, Phys. Rev. Lett. **91**, 017202 (2003).
[33] C. H. Xu, C. L. Fu, and D. F. Pedraza, Phys. Rev. B **48**, 13273 (1993).
[34] B. W. Smith and D. E. Luzzi, J. Appl. Phys. **90**, 3509 (2001).
[35] A. J. R. da Silva, A. Fazzio, and A. Antonelli, Nano Lett. **5**, 1045 (2005).
[36] V. H. Crespi, M. L. Cohen, and A. Rubio, Phys. Rev. Lett. **79**, 2093 (1997).